RSC Applied Polymers

PAPER

View Article Online
View Journal

Cite this: DOI: 10.1039/d6lp00113k

Reinforced saloplastic anion exchange membranes: balancing ionic transport and mechanical stability

Hestie A. Brink,[a,b] Jeffery A. Wood, [a] Saskia Lindhoud [b] and Wiebe M. de Vos *[a]

Developing anion exchange membranes (AEMs) that combine affordability, high conductivity, chemical stability and durability is critical to the practical implementation of many electrochemical processes. Saloplastic AEMs based on polyelectrolyte complexes of poly(styrenesulfonate) (PSS) and poly(diallyldimethylammonium chloride) (PDADMAC) meet several of these criteria, offering low-cost fabrication, good alkaline stability, and the additional advantage of sustainable processing. A major remaining challenge in the development of saloplastic AEMs is achieving sufficient mechanical stability. In the present study, this limitation was addressed by reinforcing saloplastic AEMs with woven mesh supports for the first time. To mitigate conductivity losses from non-conductive reinforcements, membrane thickness was reduced using a spacer-free hot-pressing approach, in which the apparent viscosity of the polyelectrolyte complex was tuned by salt concentration. This strategy allowed the fabrication of thin, mechanically stable and defect-free membranes, thereby minimising membrane area resistance. Reinforcements spanning a range of thicknesses and open areas were systematically investigated to decouple their effects on mechanical and transport properties. While thinner reinforcements minimised area resistance, a lower reinforcement open area strongly enhanced tensile strength with only a minor impact on ionic conductivity. Guided by these findings, a thin reinforcement with a 22% open area was selected to improve mechanical stability, increasing the tensile strength from 1.1 ± 0.2 MPa for the non-reinforced membrane to 62 ± 2 MPa. Furthermore, a substantial reduction in membrane thickness resulted in ~30% lower area resistance compared to the non-reinforced membrane. Overall, this work demonstrates that saloplastic membrane properties can be tailored to specific applications by tuning reinforcement architecture and membrane thickness to balance mechanical stability and ionic transport.

Received 1st April 2026,
Accepted 4th June 2026

DOI: 10.1039/d6lp00113k

rsc.li/rscapplpolym

1. Introduction

Ion exchange membranes (IEMs) are essential components in a wide range of electrochemical technologies, including fuel cells, electrolysers, redox flow batteries and electrodialysis stacks, by allowing selective transport of ions between different compartments.[1,2] Ideally, IEMs should be highly conductive, selective, sustainable, chemically and mechanically stable. However, these properties are strongly interdependent and improvements in one often come at the expense of others.[2–4] Membrane development therefore requires careful balancing of these trade-offs to meet the requirements of specific applications.

Alkaline electrochemical technologies, particularly alkaline fuel cells and alkaline water electrolyser systems, have attracted renewed attention due to their potential to significantly reduce costs through the use of non-precious metal catalysts.[5–10] Operation under alkaline conditions is enabled by anion exchange membranes (AEMs), which facilitate hydroxide ion transport while separating reactive compartments. Despite their promise, the development of high-performance AEMs remains challenging. Compared to commercial cation exchange membranes, AEMs typically exhibit lower ionic conductivity (due to the difference in hydroxide *vs.* proton conductivity) and reduced chemical stability, especially under harsh alkaline conditions.[10,11] These limitations have restricted their broader implementation and highlight the need for alternative AEM materials that combine efficient ion transport with sufficient chemical and mechanical stability.

Previous studies have shown that sustainable, chemically stable AEMs can be fabricated from polyelectrolyte complexes (PECs) formed by PSS and PDADMAC.[12,13] Processing of these

[a]*Department of Membrane Science and Technology, University of Twente, Enschede, Netherlands. E-mail: w.m.devos@utwente.nl*
[b]*Department of Molecules and Materials, University of Twente, Enschede, Netherlands*

materials relies on their saloplastic behaviour, which requires the presence of salt to disrupt ionic crosslinks between oppositely charged groups.[14,15] In combination with water and elevated temperature, salt plasticises the complex to enable hot-pressing into dense, freestanding membranes without the use of organic solvents.[16] This plasticisation is reversible, allowing the membranes to be recycled by salt doping and subsequent hot-pressing, making this approach even more attractive from a sustainability perspective.[17,18] Additionally, PSS-PDADMAC membranes show good chemical stability under both acidic and alkaline conditions, as long-term exposure in 1 M NaOH and 1 M H_2SO_4 showed no significant changes in their properties,[12] making them good candidates for AEMs and relevant to develop further.

Building on this foundation, our earlier work focussed on enhancing the fixed charge density of these saloplastic membranes by exploiting the tendency of the PSS-PDADMAC system to overcompensate with PDADMAC.[19] By systematically varying the degree of overcompensation, a composition with 30 mol% excess PDADMAC (based on monomer repeat units) was identified as the maximum level that provides the highest fixed charge density while remaining compositionally stable. This stability was evidenced by the absence of polyelectrolyte leaching and unchanged performance over time. Optimisation of the fixed charge density led to an 80% increase in ionic conductivity, accompanied by a moderate improvement in permselectivity, compared to previously reported PSS-PDADMAC membranes. However, this optimisation also led to increased swelling and elasticity of the membranes, revealing a critical trade-off between ionic transport and mechanical stability that limits the practical applicability of freestanding PSS-PDADMAC saloplastic AEMs.[19]

Mechanical reinforcement is a well-established strategy to address mechanical limitations in IEMs.[4,20,21] A range of reinforcement architectures, such as woven fabrics,[21–23] nonwoven mats,[4,24,25] fibrous supports,[26–28] and pore-filled structures,[29,30] have been investigated to improve mechanical strength and dimensional stability. Among these, woven reinforcements are particularly attractive because their structure is well defined and reproducible, which allows better control over parameters such as wire diameter, fabric thickness and open area. Many commercial AEMs incorporate woven reinforcement layers, including Neosepta AHA and PTFE-reinforced Sustainion X37-50, underscoring the practical importance of reinforcement for membrane durability.[20,31]

However, reinforcement also introduces additional complexity to membrane design. Because reinforcement fabrics are non-conductive, they occupy volume and partially block ion-transport pathways, thereby reducing ionic conductivity and increasing area resistance.[4,20,32] The extend of this effect depends strongly on the structure of the reinforcement fabric and on how it interacts with the polymer. Despite their widespread use in commercial membranes, relatively few studies have systematically investigated how individual reinforcement parameters affect membrane performance, which is essential information enabling reinforcement selection for specific applications.

In this study, we systematically investigate reinforced PSS-PDADMAC saloplastic AEMs with the aim of understanding and optimising key reinforcement-related trade-offs. A new spacer-free hot-pressing approach was developed to allow membrane thickness to be controlled through the combined effects of reinforcement thickness and PEC apparent viscosity. This enabled the fabrication of reinforced membranes over a wide thickness range and allowed the effect of membrane thickness on mechanical strength, swelling behaviour, permselectivity and area resistance to be examined. The influence of reinforcement open area was then studied independently to assess its role in mechanical stability and ionic conductivity. Finally, insights from these studies were used to guide the selection of reinforcement structures for the fabrication of improved PSS-PDADMAC saloplastic AEMs.

2. Materials and methods

2.1 Materials

Poly(sodium 4-styrenesulfonate) (PSS, MW = 1000 kg mol^{-1}), poly(diallyldimethylammonium chloride) (PDADMAC, MW 400–500 kg mol^{-1}), potassium bromide (KBr, ACS reagent grade ≥99.0%) and potassium chloride (KCl, ACS reagent grade, 99.0–100.5%) were purchased from Sigma Aldrich. MilliQ water was supplied by a Millipore Synergy® Water Purification System.

To enable systematic study of reinforcement parameters, woven mesh fabrics were purchased from Franz Eckert GmbH (Waldkirch, Germany). A broad material range was chosen to allow for studying the effect of reinforcement thickness while maintaining a constant open area, as well as to investigate open area using reinforcements manufactured from the same wire (constant wire thickness). Precision woven fabrics engineered specifically for reinforcement applications and made from more chemically stable materials were provided free of charge by Sefar® IEM (Heiden, Switzerland). A summary of reinforcement fabrics used in this study is given in Table 1.

2.2 Polyelectrolyte complexation

In a previous study, we optimised the fixed charge density of PSS-PDADMAC saloplastic AEMs by controlling the degree of overcharging with PDADMAC during the complexation step.[19] The best performing PEC from that study, produced from 30 mol% excess PDADMAC (based on monomer repeat units), was used in the present work.

To attempt to isolate the effect of reinforcements on membrane properties, we prepared one large batch of PEC for all membranes. Since complexation is difficult to control in large quantities, this batch was produced by preparing eight separate PEC batches (10 g calculated dry mass each) under identical conditions and later combining them.

For each batch, stock solutions of PSS and PDADMAC were prepared in 125 mM KBr. The PSS solution was prepared at a concentration of 120 mM with a total volume of 200 mL, while the PDADMAC solution was prepared at a concentration of

Table 1 Woven mesh fabrics specifications from suppliers[33,34]

Supplier: product	Material	Mesh opening (μm)	Open area (%)	Wire diameter (μm)	Fabric thickness (μm)
Eckert: PA-150/50	Polyamide	150	50	62	95
Eckert: PA-120/49	Polyamide	120	50	51	80
Eckert: PA-90/49	Polyamide	90	50	39	60
Eckert: PA-64/45	Polyamide	64	45	33	50
Eckert: PA-41/31	Polyamide	41	31	33	50
Eckert: PA-31/24	Polyamide	31	24	33	55
Eckert: PK-35/22	Polyether ether ketone	35	22	38	71
Sefar IEM 17-195/70C	Polyether ether ketone	195	70	—	40
Sefar IEM 25-195/70	Polyphenylene sulphide	195	70	—	60

156 mM with a total volume of 200 mL. These concentrations correspond to a 30 mol% excess of PDADMAC relative to PSS and a total polyelectrolyte concentration of 25 g L^{-1}.[12,19] The solids content of both polyelectrolytes was verified gravimetrically, as we found that it varies between batches and can affect the accuracy of the intended stoichiometry.

The PSS and PDADMAC stock solutions were then combined simultaneously in a third beaker under stirring, following previous studies that demonstrated this procedure yields reproducible complexation.[16,18] The mixture was stirred for an additional 15 minutes to form a solid PEC. All PEC batches were subsequently washed with Milli-Q water, oven-dried, ground to a powder and combined to form a single large batch of dried PEC.

The composition of the combined PEC batch was determined by ^{1}H-NMR, as described previously,[19] yielding a PDADMAC molar excess of ~31 ± 1% (based on monomer repeat units), which corresponds to a fixed charge density of approximately 0.6 mol L^{-1} when accounting for PEC swelling.

2.3 Membrane preparation

Reinforced saloplastic membranes were prepared using a slightly modified version presented previously for hot-pressing IEMs to give better control over membrane thickness.[19] Two grams of PEC powder was soaked in the desired salt solution (0.3, 0.5, or 0.7 M KBr) for a minimum of 24 hours. The hydrated PEC was then removed from the solution, dabbed with tissue to remove excess water, and weighed to determine the moisture content.

Delrin plates (15 × 8 × 0.5 cm^3) were used as the hot-pressing mould. For the control membranes (non-reinforced), 122 μm thick PTFE coated fibre glass spacers (Lubriglas-CHAP-1540, Reichelt Chemietechnik GmbH + Co, Heidelberg, Germany) were fixed to the bottom plate to control the thickness of the membrane, as described in our previous work (Fig. S1a in SI).[12,19] For the reinforced membranes, no spacers were used. Instead, the reinforcement fabric (cut slightly larger than the Delrin plate) was placed on the bottom plate, and the hydrated PEC was placed on top of the reinforcement as a small lump positioned in the centre (Fig. S1b in SI). The assembly was then covered with the top Delrin plate and placed directly into the preheated (90 °C) hotpress (FV20R Rollie Driptech Rosin Press, FVR, Canada). The plates were positioned so that the top Delrin plate contacted the upper heating plate, allowing the PEC to heat up without being compressed. The hot press was held in this position for 20 minutes to allow the PEC to plasticise at 90 °C.

After plasticisation, the press was slowly closed until a pressure of 150 bar was reached and held for an additional 15 minutes. Heating was then switched off and the PEC was allowed to cool to room temperature under pressure. Once cooled, the press was opened and the membrane was removed from between the Delrin plates.

Five test membranes (2 × 2 cm^2) were cut from each membrane and soaked in 50 mL of 0.5 M KCl to equilibrate. Test membranes were equilibrated for at least 7 days, and the equilibration solution was refreshed at least twice before testing, as membranes pressed at 0.7 M KBr required longer equilibration times to reach stable results.

2.4 SEM

Scanning electron microscopy (SEM) was used to study the morphology of the reinforced saloplastic films using a JSM-6010LA instrument (JEOL, Japan). Prior to SEM analysis, the membranes were first air-dried and cut to the required size using a sharp razor blade. The samples were then mounted on SEM stubs and dried under vacuum at 30 °C overnight to remove residual moisture. The dried samples were subsequently coated with a 5 nm Pt/Pd layer using a Quorum Q150T ES sputter coater (Quorum Technologies Ltd, UK). SEM images were obtained from the top surface, bottom surface and cross sections of the films to check whether the films were dense, identify defects and examine the adhesion between the reinforcement fabric and the PEC.

2.5 Thickness

The wet thickness (t_{wet}) of each equilibrated test membrane was measured using a micrometer. Five test membranes were cut from the original membrane and the thickness of each was measured. The reported wet thickness corresponds to the average thickness of the five test membranes, with the 95% confidence interval as error.

2.6 Swelling

Water uptake and swelling ratio (in length and thickness) were tested to evaluate the swelling behaviour of the saloplastic

membranes. Membrane samples, equilibrated in 0.5 M KCl at room temperature, were cut into 4 × 1 cm^2 ($l_{wet} \times w_{wet}$) strips using a razor blade. The membranes were blotted dry with a tissue paper and then weighed and measured to obtain the wet weight (w_{wet}), wet length (l_{wet} = 4 cm) and the wet thickness (t_{wet}). The membrane strips were placed between Delrin plates to prevent curling during drying, and placed in an oven at 105 °C for 3 hours. The samples were then weighed and the dimensions measured to obtain the dry weight (w_{dry}), dry length (l_{dry}) and the dry thickness (t_{dry}). The water uptake (WU), swelling ratio length (SR_{length}) and swelling ratio thickness ($SR_{thickness}$) was calculated and reported as the average of a minimum of three measurements with the 95% confidence interval as error.[1,35]

$$WU\,(\%) = \frac{w_{wet} - w_{dry}}{w_{dry}} \times 100\%,$$

$$SR_{length}\,(\%) = \frac{l_{wet} - l_{dry}}{l_{dry}} \times 100\%,$$

$$SR_{thickness}\,(\%) = \frac{t_{wet} - t_{dry}}{t_{dry}} \times 100\%.$$

For reinforced membranes, the water uptake and through-plane swelling ratio of the PEC phase were also calculated by correcting for the reinforcement mass (w_{reinf}) and thickness (t_{reinf}). For this correction, the dry weight and thickness of a 4 × 1 cm^2 reinforcement sample were measured separately. The water uptake of the PEC phase (WU_{PEC}) and the through-plane swelling ratio of the PEC layer ($SR_{thickness,\,PEC}$) were then calculated as follows:

$$WU_{PEC}\,(\%) = \frac{w_{wet} - w_{dry}}{w_{dry} - w_{reinf}} \times 100\%,$$

$$SR_{thickness,\,PEC}\,(\%) = \frac{t_{wet} - t_{dry}}{t_{dry} - t_{reinf}} \times 100\%.$$

2.7 Mechanical strength

Stress–strain curves were obtained from an electromechanical testing system (Instron 5800), operating at a speed of 2 mm min^{-1} at room temperature. Membrane samples (5 × 50 mm^2 strips) were prepared according to the ASTM D882 standard for thin (<1 mm) polymer films.[36] A minimum of three measurements on separate samples were taken for each data point.

2.8 Water transport

Water transport measurements were performed using a diffusion cell in which an IEM (diameter 5 cm, exposed area 19.6 cm^2) separated two compartments containing KCl solutions of different concentrations (0.1 M and 0.5 M). The total liquid volume in each compartment, including a connected graduated pipette used as a level indicator, was approximately 80 mL.

Each compartment contained a magnetic stir bar to continuously mix the solution adjacent to the membrane surface. Changes in liquid volume were monitored using the graduated pipettes (mL scale) connected to each compartment. After filling and initiating stirring, initial pipette readings were recorded (t = 0), and volume changes were recorded at regular time intervals over 8 hours. Water transport was quantified as water flux, calculated from the total change in pipette volume ($V_2 - V_1$) over time ($t_2 - t_1$) and normalised by the membrane area (A). Experiments were conducted at room temperature, and selected membranes were tested in duplicate.

$$\text{Water flux}\,(\text{mL m}^2\,\text{h}) = \frac{(V_2 - V_1)}{(t_2 - t_1) \times A}.$$

2.9 Permselectivity

Permselectivity was evaluated by measuring the membrane potential generated under an imposed ionic concentration gradient. Membrane samples were mounted between two compartments containing KCl solutions of 0.1 M (low concentration side) and 0.5 M (high concentration side). The electrolyte solutions were continuously circulated through a thermostatic bath to maintain a constant temperature of 25 °C.

Ag/AgCl reference electrodes positioned in close proximity to the membrane surfaces in each compartment were used to measure the resulting potential difference across the membrane.

Permselectivity was calculated as the ratio of the experimentally measured potential difference ($\Delta\varphi_{measured}$) to the theoretical Nernst potential ($\Delta\varphi_{Nernst}$):

$$\text{Permselectivity}\,(\%) = \frac{\Delta\varphi_{measured}}{\Delta\varphi_{Nernst}} \times 100\%$$

$$\Delta\varphi_{Nernst} = \frac{RT}{zF} \ln \frac{C_2\gamma_2}{C_1\gamma_1}$$

where R is the universal gas constant, T the absolute temperature, z the ionic valence, F the Faraday constant, C_1 and C_2 the electrolyte concentrations (0.1 and 0.5 M, respectively), and γ_1 and γ_2 their corresponding activity coefficients. Reported values represent the mean of at least five independent measurements, with the 95% confidence interval indicated as the error.

2.10 Area resistance

The ionic resistance of the membranes was measured using a six-compartment Plexiglas cell, as described previously.[19,37,38] The test membrane was placed between the two central compartments, which were circulated with 0.5 M KCl. The adjacent compartments were also circulated with 0.5 M KCl, while the outermost compartments, containing the platinum-coated titanium electrodes, were circulated with 0.5 M K_2SO_4. Haber-Luggin capillaries connected to Ag/AgCl reference electrodes (VWR, The Netherlands) were positioned on opposite sides of the membrane, facing each other, to measure the voltage drop across the membrane.

Stepwise currents from 0 to 15 mA were applied using a Metrohm Autolab potentiostat (PGSTAT302N, The Netherlands), and the resulting current–voltage curve was used

to determine the total system resistance. The area resistance of the membrane (R_{area}) was calculated by subtracting the solution resistance ($R_{solution}$) and multiplying by the membrane area (A = 1.77 cm^2).

The area resistance of the membrane (R_{area}) and ionic conductivity (σ) were calculated as:[37,38]

$$R_{area}\ (\Omega\ \mathrm{cm}^2) = (R_{total} - R_{solution}) \times A$$

$$\sigma\ (\mathrm{mS\,cm}^{-1}) = \frac{t_{wet}}{R_{area}}$$

where t_{wet} is the membrane thickness measured with a micrometer. Both area resistance and ionic conductivity are reported as the average of five measurements, with the 95% confidence interval indicated as the error margin.

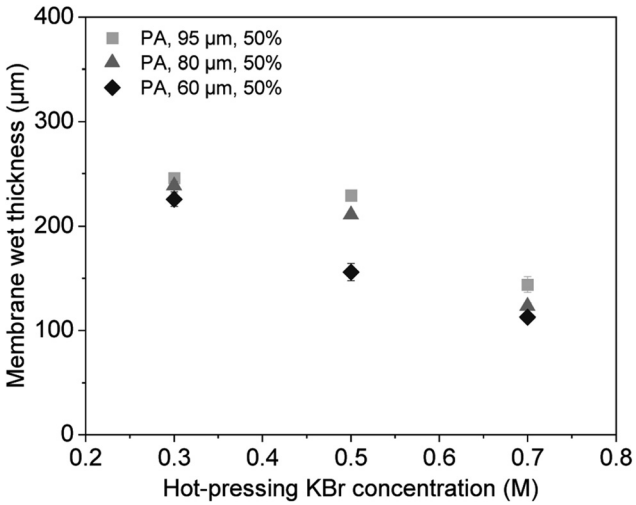

Fig. 1 Wet thickness of reinforced saloplastic membranes (measured in 0.5 M KCl) as a function of the KBr concentration used during hot-pressing. Data are shown for membranes fabricated with three polyamide (PA) woven reinforcements of different fabric thicknesses and similar open areas. Legend entries are given as (reinforcement material, fabric thickness, open area). Each data point represents the average thickness of five specimens cut from a single pressed membrane, with error bars showing the 95% confidence interval. Note that some error bars were smaller than the marker and are therefore not visible.

3. Results and discussion

3.1 Fabrication and thickness control of reinforced saloplastic AEMs

In previous work, the hydrated PEC was placed between Delrin press plates separated by fixed PTFE-coated fiberglass spacers during hot-pressing.[12,19] These spacers formed a mould with a defined gap that controlled the membrane thickness. In the present study, these spacers were removed to enable the fabrication of reinforced membranes. This spacer-free configuration enables a fundamentally different route to membrane thickness control compared to conventional spacer-defined hot-pressing methods. The reinforcement fabric with the hydrated PEC placed on top was pressed between two Delrin plates, as shown in Fig. S1 in the SI. As a result, the thickness of the reinforced membranes was no longer set by the spacer height, but instead determined by the thickness of the reinforcement fabric and the apparent viscosity of the PEC. In this work, apparent viscosity refers to the resistance to flow of this plasticised, soft, viscoelastic material.

Using this spacer-free hot-pressing approach, the first part of this study focused on modifying membrane thickness to investigate its effect on membrane properties. To achieve this, three polyamide (PA) reinforcements with similar open areas (50%) but different fabric thicknesses (60, 80 and 95 μm) were selected (see Table 1 for specifications). In this study, reinforced membranes are labelled by the properties of the reinforcement, given as (material, fabric thickness, open area).

The thickness of the PEC layer was adjusted by equilibrating dried PEC powder in solutions with varying salt concentrations (0.3, 0.5 and 0.7 M KBr) prior to hot-pressing. This works because salt plasticises the PEC by screening electrostatic interactions and breaking ionic crosslinks during the heating step.[14,15,19] Consequently, at higher salt concentrations, the apparent viscosity of the PEC is reduced, resulting in thinner membranes once pressed.

The effectiveness of this approach is clearly demonstrated in Fig. 1, which shows a decrease in membrane thickness with increasing PEC salt concentration and decreasing reinforcement thickness. The error bars represent the variation in thickness across specimens cut from a single pressed membrane. Although a reduction in thickness is observed for all reinforcement types, the trend is not consistent between reinforcements, with the thinnest fabric (60 μm) showing the most pronounced decrease. Hot-pressing of plasticised PEC is sensitive to processing conditions, therefore, precise control over membrane thickness remains challenging. Further optimisation of the process is therefore required. Nevertheless, the overall downward trend confirms that salt concentration can be used as a tuning parameter to control membrane thickness.

SEM was used to examine the membrane structure and adhesion between the PEC layer and the reinforcement. Representative SEM images of membranes prepared using the thinnest PA reinforcement (60 μm) and PEC equilibrated in 0.3, 0.5 and 0.7 M KBr solutions are shown in Fig. 2a–c, respectively. For each salt concentration, images of the cross-section (left), top-surface (middle) and bottom-surface (right) are presented.

The cross-sectional images show a distinct PEC layer on top of the reinforcement for all membranes, with the PEC layer becoming thinner as the equilibration salt concentration increases. The indicated thickness values correspond to the dry membrane thickness, as SEM analysis was performed on dried samples. Good adhesion between the PEC layer and the reinforcement is observed in all cases, with no signs of delamination. However, long-term interfacial stability under extended operation remain to be evaluated in future work.

The top surface images show dense PEC layers without visually observable defects. For the membrane prepared using 0.7

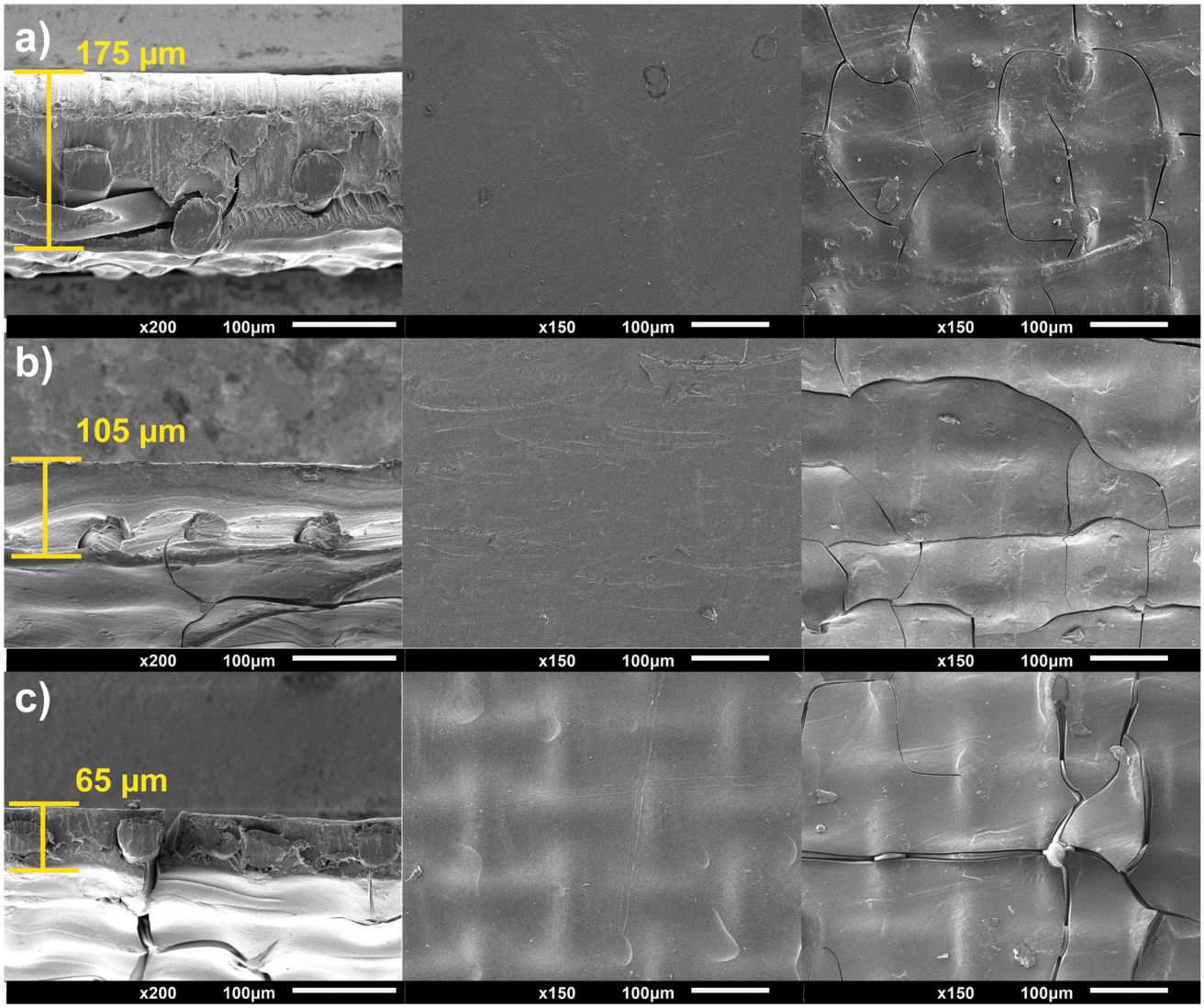

Fig. 2 SEM images of dry reinforced saloplastic membranes fabricated using the thinnest polyamide reinforcement (60 µm fabric thickness). Cross-sectional (left), top-surface (middle) and bottom-surface (right) images are shown for membranes hot-pressed using PEC equilibrated in (a) 0.3 M KBr, (b) 0.5 M KBr and (c) 0.7 M KBr.

M KBr (Fig. 2c), the reinforcement mesh is faintly visible at the surface, indicating that the PEC layer is very thin while still providing full surface coverage. The bottom surface images show that the PEC largely fills and covers the reinforcement after hot-pressing, although small areas of exposed mesh are visible. This is expected since PEC was placed on top of the reinforcement and pressed down into the mesh openings without PEC present below the reinforcement to completely cover that surface. Nevertheless, because the mesh openings are filled and the top surface is fully covered, overall membrane integrity is preserved.

To illustrate the mechanical enhancement provided by woven mesh reinforcement, Fig. 3 shows the stress–strain response of reinforced membranes compared to a non-reinforced membrane (PEC only), together with the response of the reinforcement fabric. Only membranes fabricated using the thinnest reinforcement (PA, 60 µm) are shown, as these are representative of all trends. The stress–strain curves of the other reinforcement fabrics are provided in the SI (Fig. S2a). The non-reinforced membrane exhibits low mechanical strength and a much higher elongation at break. In contrast, the reinforcement fabric alone displays a steep stress–strain curve, characteristic of a woven mesh.[23,39,40]

The comparison with the non-reinforced PEC membrane indicates that the reinforcement fabric is the dominant load-bearing component of the composite, as the PEC alone exhibits significantly lower mechanical strength and a distinctly different stress–strain response. In contrast, reinforced membranes show behaviour more closely resembling that of the reinforcement fabric, suggesting that the overall mechanical response is primarily governed by the woven mesh. Reinforced membranes nevertheless show intermediate behaviour, with

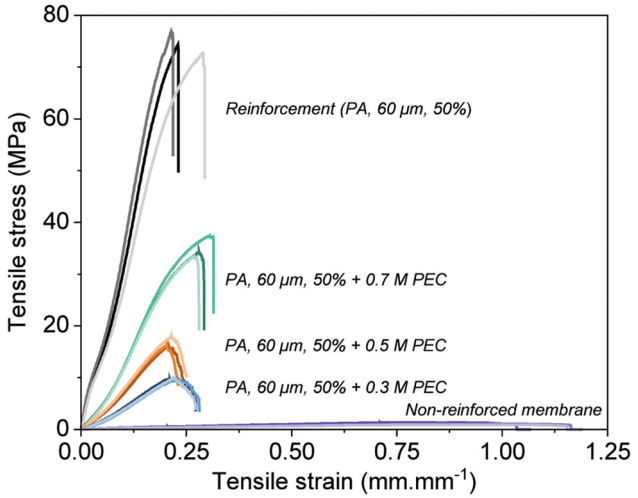

Fig. 3 Tensile stress–strain curves of reinforced saloplastic AEMs prepared using the same polyamide (PA) woven reinforcement (60 µm fabric thickness, 50% open area) and different PEC layer thicknesses, obtained by equilibrating the PEC in 0.3, 0.5 and 0.7 M KBr prior to hot-pressing. The response of the reinforcement fabric alone and the non-reinforced membrane (PEC only) is shown for comparison. Three repeat measurements are shown for each membrane.

the contribution of the reinforcement becoming more pronounced as the PEC layer thickness decreases. Although thickness normalisation complicates quantitative comparison of tensile stress in composite materials, the observed trends suggest that the mechanical behaviour of the reinforced membranes is largely governed by the reinforcement. The corresponding load-strain curves without thickness normalisation are provided in the SI (Fig. S2b).

Overall, reinforcements greatly enhanced the mechanical strength of the membranes, converting the weak, highly deformable PEC into a strong, reinforcement-dominated composite membrane. By carefully controlling reinforcement thickness and the PEC hot-pressing viscosity, membranes were fabricated as thin as possible, which limits the trade-off between mechanical strength and ionic resistance.

3.2 Effect of membrane thickness on membrane properties

3.2.1 Swelling behaviour as a function of membrane thickness. Our previous work showed that PSS-PDADMAC saloplastic AEMs swell considerably and deform during performance testing, motivating the use of mechanical reinforcement.[19] Reinforcement of IEMs is commonly reported to reduce swelling by limiting polymer chain mobility and suppressing deformation.[20,41] To evaluate this, water uptake and in-plane (SR length) and through-plane (SR thickness) swelling ratios of reinforced membranes were measured and compared to non-reinforced saloplastic membranes. To focus on the intrinsic swelling behaviour of the PEC, water uptake and SR thickness are reported for the PEC phase only. Swelling results of the overall composite membrane (PEC + reinforcement) show a thickness dependence arising from the polymer-to-reinforcement ratio rather than from interactions between the polymer and the reinforcement and are therefore less relevant for this study. For completeness, results for the overall reinforced membranes are provided in Fig. S3 in the SI.

Fig. 4 shows the water uptake of the PEC phase as a function of membrane thickness for both reinforced and non-reinforced membranes. Within experimental uncertainty, the water uptake is the same for reinforced and non-reinforced membranes and shows no dependence on membrane thickness. To better understand this behaviour, in-plane (SR length) and through-plane (SR thickness) swelling ratios were examined and are shown in Fig. 5. The swelling ratios were calculated as the relative change in dimension (length and thickness) between the hydrated and dry states. The dry thickness of non-reinforced membranes could not be reliably measured due to brittleness and curling of samples; therefore, SR thickness values for non-reinforced membranes are not included.

As shown in Fig. 5a, the SR length of the PEC layer is relatively low (~8%) for all membranes and shows no discernible dependence on reinforcement or membrane thickness. Similarly, Fig. 5b shows that the SR thickness of the PEC layer, calculated as described in see section 2.6, is largely independent of both reinforcement and membrane thickness. These results are consistent with the water uptake data and indicate that reinforcement does not significantly restrict PEC swelling, even when mechanical properties (specifically elastic modulus) have greatly increased.

This behaviour contrasts with literature reports, which typically show that incorporation of a mesh restricts water transport and polymer expansion.[20,22,41] If strong interactions between the PEC and the reinforcement were present, a reduction in SR length would be expected for reinforced membranes, along with lower PEC water uptake. In addition,

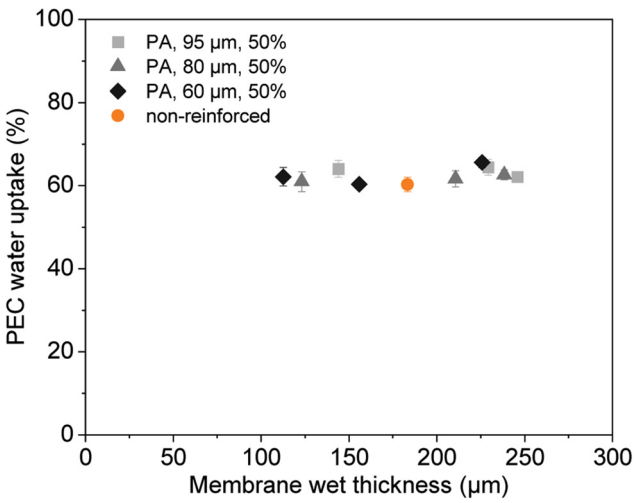

Fig. 4 Water uptake of the PEC fraction as a function of wet membrane thickness for reinforced saloplastic AEMs with systematically varied thicknesses. Data for a non-reinforced membrane (PEC only) are included for comparison. Error bars represent the 95% confidence interval (n = 5).

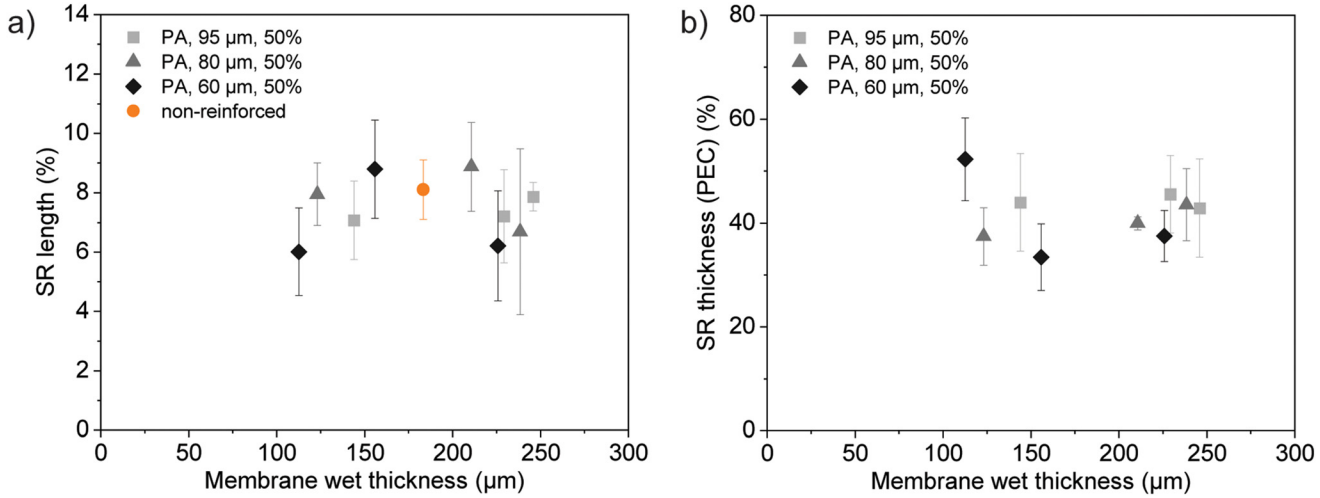

Fig. 5 Swelling ratio of saloplastic AEMs as a function of wet membrane thickness: (a) in-plane swelling (SR length) and (b) through-plane swelling (SR thickness, PEC layer only). Data for a non-reinforced membrane (PEC only) are included for comparison. Error bars represent the 95% confidence interval (n = 5).

thinner PEC layers would be expected to swell less than thicker layers due to a larger fraction of the polymer being in close contact with the reinforcement, leading to a thickness dependence of SR thickness. None of these trends are observed in our study.

One possible explanation is that the reinforcing mesh is too open or flexible to effectively constrain polymer swelling. In addition, swelling of the PSS-PDADMAC membranes occurs predominantly in the through-plane direction, with SR thickness (~40%) being much larger than the in-plane swelling (~8%), even in non-reinforced membranes. Since the reinforcement is primarily expected to restrict in-plane expansion, the comparatively low in-plane swelling may explain why reinforcement does not lead to a measurable reduction in PEC swelling.

3.2.2 The effect of membrane thickness on ion transport. Membrane thickness is an important parameter to consider when optimising IEM performance, as reducing thickness lowers the area resistance without significantly affecting permselectivity. Permselectivity is generally considered to be independent of membrane thickness, provided that the membranes do not contain any through-thickness defects.[42–44] Having confirmed that the reinforced membranes of all thicknesses are visually free of defects (see Fig. 2), the effect of membrane thickness on ion transport properties was examined next.

Fig. 6a shows the area resistance of non-reinforced and reinforced membranes as a function of wet membrane thickness. As expected, the area resistance of reinforced membranes is higher than that of non-reinforced membranes of a similar thickness since the woven mesh is non-conductive.[20,22] Moreover, we find that the resistance scales almost linearly with membrane thickness, although a slight deviation (higher resistance) is observed for thinner membranes. Extrapolation of the resistance-thickness trend gives an intercept close to zero, suggesting that no other resistances or impedances, such as boundary layer effects, were present under the applied test conditions.

The ionic conductivity (thickness-normalised) of the same membranes is shown in Fig. 6b. Conductivity values for non-reinforced membranes show larger uncertainty, as these membranes deform during testing (see Fig. S4 in SI). Stretching during the measurement reduces the membrane thickness and therefore the measured resistance, whereas the thickness is determined after the test when the membrane has partially recovered. As conductivity is calculated by normalising resistance by thickness,[37,38] this can lead to an overestimation of conductivity for non-reinforced membranes. Consequently, the actual difference in conductivity between reinforced and non-reinforced membranes is likely smaller than suggested by the measured values. This is encouraging, as it shows that reinforcement can be introduced to saloplastic membranes with only a limited impact on ionic transport.

The conductivity results also confirm that the thinnest reinforced membranes (prepared using 0.7 M KBr) are free of through-thickness defects, as no increase in conductivity is observed for thinner membranes.[29,32] This observation is consistent with the absence of visible defects in the SEM images (Fig. 2). The slightly lower conductivity observed for thinner membranes is expected, as they contain a higher fraction of non-conductive reinforcement relative to conductive PEC.

To explore whether the ionic conductivity of the reinforced saloplastic AEMs can be expressed as a function of the polymer-reinforcement ratio, ionic conductivity was analysed as a function of PEC content (Fig. 7a), defined as the mass fraction of PEC relative to the combined mass of PEC and reinforcement. A dashed line is included to indicate the expected linear scaling between the conductivity of the non-reinforced membrane (100% PEC content) and zero conductivity at zero PEC content. From this graph it can be seen that membranes prepared with 0.7 M KBr, *i.e.* membranes with the

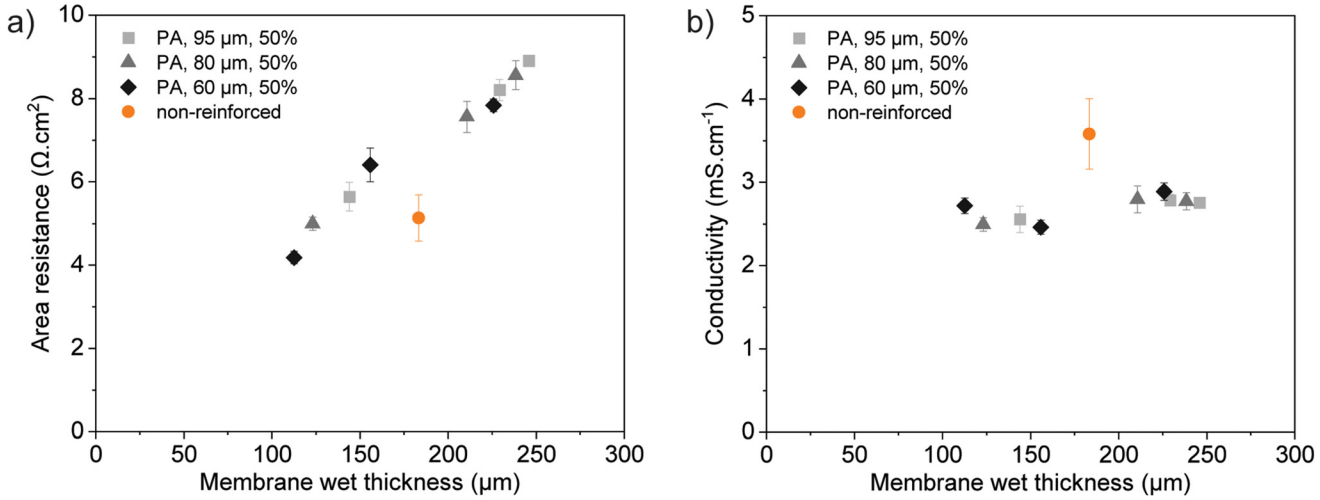

Fig. 6 Area resistance (a) and ionic conductivity (b) of saloplastic AEMs as a function of wet membrane thickness. Data for a non-reinforced membrane (PEC only) are included for comparison. Error bars represent the 95% confidence interval (n = 5).

thinnest PEC top-layers, follow the expected scaling of conductivity with PEC content more closely. In contrast, membranes with thicker PEC layers deviate from this behaviour and exhibit lower conductivities than expected based on PEC content. This suggests that PEC content alone does not fully describe ionic transport behaviour.

A likely explanation is that ion transport occurs through at least two distinct regions within the reinforced membranes, shown schematically in Fig. 7c. The first region is a dense PEC layer, which provides a relatively direct pathway for ion transport. The second region consists of the PEC-reinforcement composite, where the presence of the non-conductive reinforcement reduces the effective conductive area and introduces more tortuous transport pathways, resulting in a higher resistance. When the PEC layer is very thin, the membrane effectively behaves as a single transport region. In this case, thickness normalisation provides a reasonable approximation of the effective transport distance, which also explains why these membranes follow the expected scaling between PEC content and conductivity more closely. As the PEC layer becomes thicker, transport through the dense PEC region becomes increasingly important. Because two transport regions with different conductivities contribute to ion transport, normalising conductivity using the total membrane thickness becomes less representative of the effective transport distance. As a result, simple scaling with PEC content no longer holds.

To further evaluate this hypothesis, a simple series resistance model was considered in which the total membrane resistance is approximated as the sum of the resistances of the dense PEC layer and the PEC-reinforcement composite region. The thickness of the composite region was set equal to the thickness of the reinforcement fabric, while resistance data from non-reinforced membranes (PEC only) were used to estimate the resistance of the dense PEC layer. Details of this analysis are provided in the SI, section S5 estimation of resistance contribution of two transport regions.

Fig. 7b shows the calculated resistance contributions for the two transport regions for all reinforced membranes. The thickness of each region is indicated inside the corresponding bar in µm. The resistance of the dense PEC region scales linearly with the thickness of this layer. Importantly, the resistance contribution of the PEC-reinforcement region remains approximately constant for each reinforcement set and decreases when thinner reinforcement fabrics were used. This indicates that the series resistance model captures the general behaviour and supports the concept of two transport regions in the reinforced membranes. Deviations from perfect scaling are expected, as ion transport may also be influenced by the reinforcement architecture and transport processes occurring at the PEC-reinforcement interface.

The permselectivity of these membranes were also examined as a function of membrane thickness, as shown in Fig. 8. In our previous work, the permselectivity of saloplastic AEMs was negatively affected by low mechanical stability and high swelling.[19] Reinforcement was therefore expected to improve permselectivity by mitigating both of these limitations. As discussed in the previous sections, reinforcement enhanced mechanical stability (Fig. 3), thereby preventing membrane deformation during testing, but did not reduce the swelling of the PEC (section 3.2.1). Consequently, any observed changes in permselectivity can be attributed primarily to improved mechanical stability rather than differences in water uptake.

Consistent with this expectation, reinforced membranes show a slight improvement in permselectivity compared to non-reinforced membranes, especially for thicker membranes (Fig. 8). As illustrated in Fig. S4 of the SI, reinforced membranes maintain their shape while non-reinforced membranes stretch and deform during testing. Such deformation can lead to the formation of small defects that reduce permselectivity

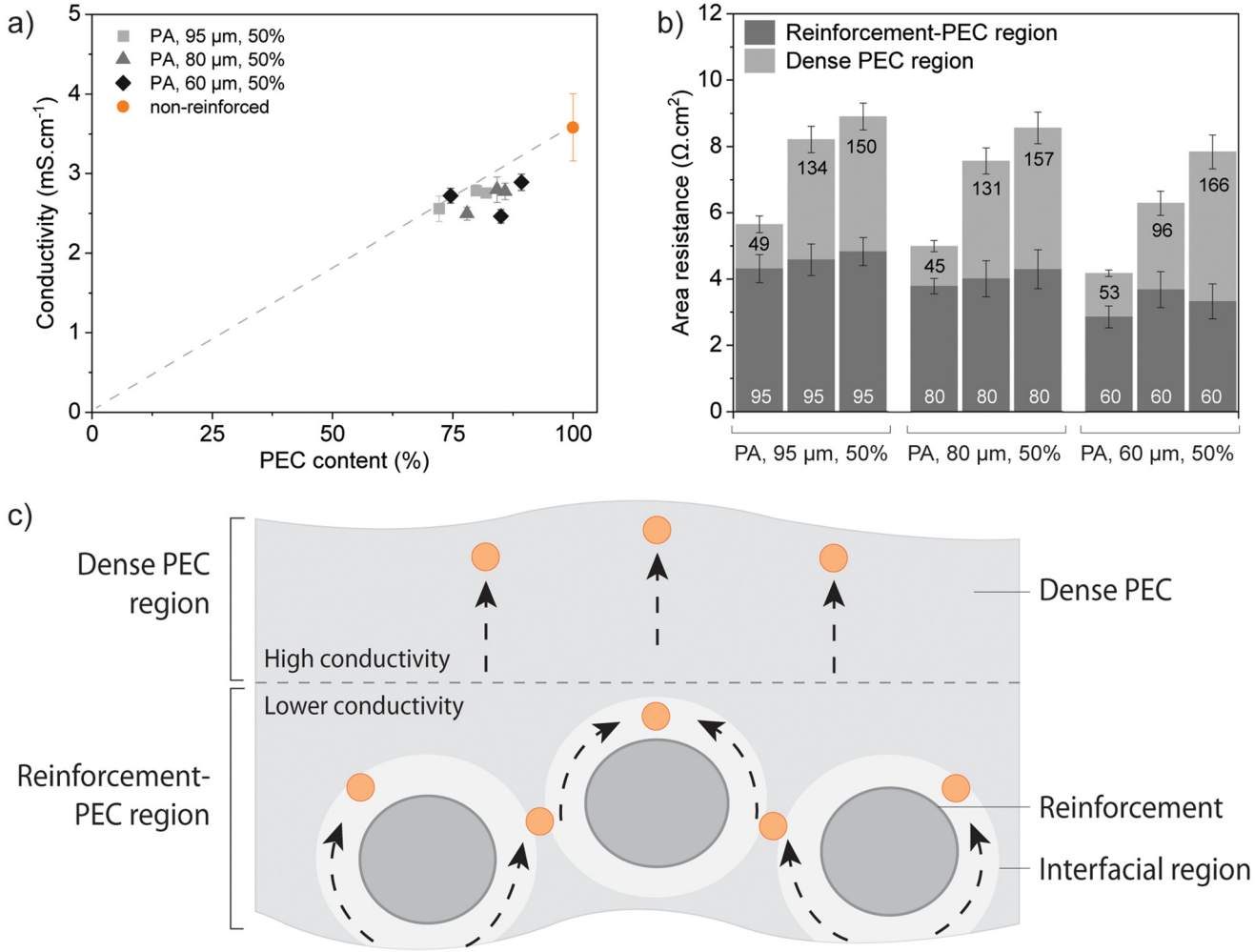

Fig. 7 (a) Ionic conductivity of reinforced saloplastic membranes as a function of PEC content. The dashed line indicates the expected linear scaling between the conductivity of the non-reinforced membrane (100% PEC) and zero conductivity. (b) Estimated resistance contributions of the dense PEC layer and the PEC-reinforcement composite region obtained using a simple series resistance model. Numbers in the stacked bars indicate the thickness of each region (µm). (c) Schematic illustration of the proposed two transport regions in reinforced saloplastic membranes: a dense PEC layer and a PEC-reinforcement composite region. Error bars represent 95% confidence intervals.

and contribute to increased variability between samples. The lower permselectivity values observed here result from testing at 0.5 M KCl, a concentration close to the membrane's fixed charge density (~0.6 mol L^{-1}), where the Donnan effect is weakened. This testing condition was chosen deliberately, as operating near the fixed charge density makes any improvement in permselectivity easier to detect. However, previous work have shown that these membranes remain highly permselective (>90%) at lower electrolyte concentrations (0.02/0.1 M KCl).[19]

Although permselectivity in IEMs is generally expected to be independent of thickness,[42–44] Fig. 8 shows a gradual decrease in permselectivity with decreasing thickness for reinforced saloplastic membranes. This behaviour is unlikely caused by macroscopic defects, as it is inconsistent with the SEM (Fig. 2) and conductivity (Fig. 6b) results. Moreover, the reduction in permselectivity shows an approximately linear dependence on membrane thickness, rather than the highly scattered and variable results typically associated with defective membranes.

This thickness dependence of permselectivity might be explained by the significant swelling of the saloplastic membranes (Fig. 4). The measured permselectivity of IEMs reflects contributions from both ion transport and water transport, with the latter described by the water transference coefficient.[45,46] While ion transport is generally independent of membrane thickness, water transport can depend on thickness and may therefore influence the permselectivity. To investigate whether water transport contributes to the observed decrease in permselectivity with decreasing thickness, water transport experiments were performed under identical chemical potential gradient conditions as the permselectivity tests (0.1/0.5 M KCl). Due to the time-intensive nature of these measurements, the experiments were conducted only for the thinnest reinforcement (PA, 60 µm) and for membranes pre-

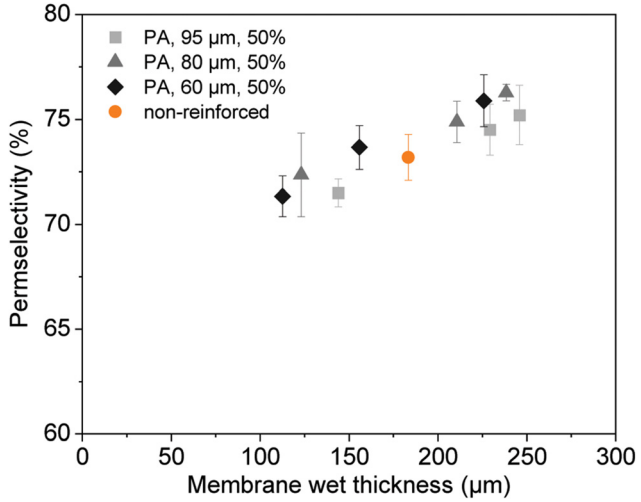

Fig. 8 Permselectivity of saloplastic AEMs as a function of wet membrane thickness. Data for a non-reinforced membrane (PEC only) are included for comparison. Error bars represent the 95% confidence interval (n = 5).

pared using the thickest and thinnest PEC layers (PECs hot-pressed with 0.3 and 0.7 M KBr), representing the extremes of the investigated thickness range. For the thinnest membrane (~100 µm), a water flux of 61 ± 9 mL m^{-2} h^{-1} was measured, whereas the thickest membrane (~220 µm) exhibited a substantially lower water flux of 12 ± 5 mL m^{-2} h^{-1}. For reference, a commercial reinforced membrane of similar thickness (216 µm), Neosepta AHA, was measured to have a water flux of 4.2 ± 1.2 mL m^{-2} h^{-1}, confirming the relatively hydrophilic nature of saloplastic membranes. Together with the significantly higher water flux observed for the thinner membranes, this supports the hypothesis that the thickness dependence of permselectivity of the reinforced saloplastic membranes may largely be related to water transport. Future work could further investigate this by quantifying the ion transport number and water transference coefficient in these saloplastic membranes.[45]

To better understand the observed differences in water flux, the membrane structure must also be considered. The reduction in water flux does not scale linearly with membrane thickness, supporting the two-region transport concept introduced earlier (Fig. 7c). Water transport through the PEC-reinforcement composite likely differs from that through the dense PEC layer, and interfacial regions between the highly swollen PEC and the rigid reinforcement may further influence transport. While the precise mechanisms remain to be studied, these results further highlight the complex and heterogeneous transport occurring in the PEC-reinforcement region.

Overall, these results show that incorporation of woven mesh supports enables the fabrication of thinner saloplastic membranes, thereby minimising membrane area resistance. Reinforcement also leads to a modest improvement in permselectivity by enhancing dimensional stability. However, permselectivity decreases slightly with decreasing membrane thickness, which is likely due to the increased contribution of water transport in thinner membranes. Importantly, the resulting loss in permselectivity is outweighed by the substantial reduction in area resistance achieved by fabricating thinner, mechanically reinforced membranes, demonstrating that the resistance-mechanical stability trade-off can be effectively managed through thickness optimisation.

3.3 Effect of reinforcement open area on membrane properties

To investigate the effect of reinforcement open area independently of membrane thickness, all membranes in this section were fabricated using the same hot-pressing conditions with an optimised PEC salt concentration of 0.7 M KBr. Commercially available polyamide (PA) woven fabrics made from identical 33 µm diameter wires were used as reinforcements, resulting in similar membrane thicknesses across all samples. Differences in reinforcement open area therefore arise solely from variations in weave pattern, allowing the effect of open area on membrane properties to be examined independently of membrane thickness.

Fig. 9 shows the tensile strength of reinforced saloplastic membranes as a function of reinforcement open area, with the non-reinforced membrane included as a reference (100% open area). The non-reinforced membrane exhibits very low tensile strength (~1 MPa). Incorporation of woven reinforcement leads to a substantial increase in tensile strength, which increases steadily with decreasing open area. This indicates that tighter weaves provide enhanced mechanical stability, consistent with literature.[23]

The ionic conductivity of the same membranes is shown in Fig. 10a as a function of reinforcement open area. As expected,

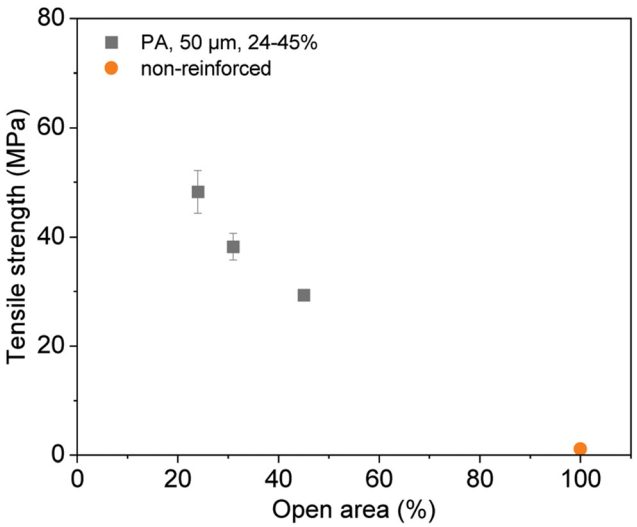

Fig. 9 Tensile strength of saloplastic AEMs as a function of reinforcement open area. Data for a non-reinforced membrane (PEC only, 100% open area) are included for comparison. Error bars represent the 95% confidence interval (n = 3).

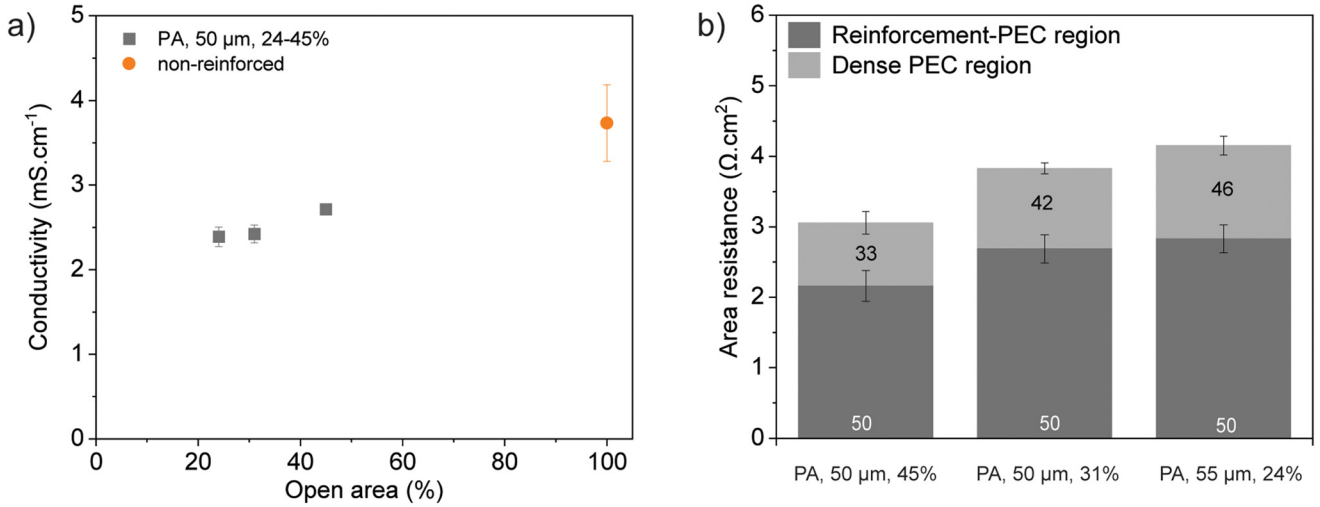

Fig. 10 (a) Ionic conductivity of saloplastic AEMs as a function of reinforcement open area. (b) Estimated resistance contributions of the dense PEC layer and the PEC-reinforcement composite region of reinforced membranes with different open areas. Numbers in the stacked bars indicate the thickness of each region (µm). Error bars represent the 95% confidence interval (n = 5).

the incorporation of non-conductive reinforcement reduces the conductivity relative to the non-reinforced membrane.[20,30,47] Within the reinforced membrane set, conductivity increases slightly with increasing open area. However, the dependence is relatively weak, decreasing only from 2.7 ± 0.1 to 2.4 ± 0.1 mS cm^{-1} when the open area is reduced from 45% to 24%. Given that these membranes were fabricated with very thin PEC top-layers, ion transport was expected to be largely dominated by the PEC-reinforcement composite region. Thus, a stronger dependence of conductivity on reinforcement open area was expected.

To explore this behaviour further, the series resistance model introduced in section 3.2.2 was applied to separate the total membrane resistance into contributions from the dense PEC layer and the PEC-reinforcement composite region. Because identical reinforcement fibres were used for all samples, the thickness of the PEC-reinforcement region was assumed to be constant, with only the weave density (and thus open area) varying. As shown in Fig. 10b, even when separating the resistance into these two regions, the resistance of the PEC-reinforcement region does not vary as strongly with open area as might be expected. Membrane resistance is typically measured and reported as area resistance, which scales linearly with membrane area (*i.e.* membrane size). By analogy, one would expect that reducing the open area of the reinforcement would proportionally reduce the conductive area of the PEC-reinforcement region, leading to a corresponding increase in resistance. However, ions can still move around the non-conductive reinforcement, creating tortuous and complex transport pathways.[20,48] This prevents a simple linear scaling with open area and highlights the intricate ion transport behaviour in this composite region.

These results reveal a surprising but highly beneficial feature: reinforcement with very low open areas can greatly increase membrane mechanical strength without imposing a proportional penalty on ionic transport. In the next section, membranes with more extreme variations in open area will be examined to further examine these effects.

3.4 Selection of reinforcements and performance trade-offs

Based on the separate investigations of reinforcement thickness and open area in the preceding sections, the following experiments combine these insights to guide the selection of reinforcements for improved saloplastic AEM performance. Section 3.2 shows that reducing overall membrane thickness is an effective strategy to lower area resistance, highlighting the importance of using thin reinforcement fabrics in addition to thin PEC layers. Section 3.3 shows that reinforcement open area introduces a trade-off between mechanical stability and ionic conductivity, with lower open areas providing substantially higher mechanical strength, while higher open areas lead to slightly higher conductivity. However, the influence of open area on ionic transport was noticeably weaker than expected. Together, these results provide a clear motivation for selecting thin reinforcements with distinctly different open areas to further explore these trade-offs.

Accordingly, thin woven reinforcements with large open areas (70%) were selected to favour ionic transport, while a reinforcement with a much lower open area (22%) was included to maximise mechanical stability. These reinforcements are based on chemically stable materials, which is an important consideration for practical membrane applications.[22,29] All membranes were fabricated using an optimised PEC salt concentration of 0.7 M KBr to minimise the thickness of the PEC top layer. Under these conditions, the dense PEC layer is expected to be very thin, meaning that ion transport is largely dominated by the PEC-reinforcement composite region. This selection allows us to examine the conduc-

tivity-mechanical stability and resistance-permselectivity trade-offs identified in the preceding sections with optimised reinforcements (Fig. 11).

Fig. 11a compares the tensile strength and ionic conductivity of these membranes. The results are consistent with the trends observed in the open area study (section 3.3). The membrane reinforced with the PEEK fabric having 22% open area exhibits a threefold increase in tensile strength compared to membranes reinforced with fabrics of 70% open area. Despite this large difference in reinforcement structure and PEC content (58% *vs.* 80%), the associated reduction in ionic conductivity (2.7 ± 0.1 *vs.* 2.4 ± 0.1 mS cm^{-1}) remains modest and not proportional to the loss in open area or PEC content. Even when considering these more extreme designs, reinforcement open area still has a surprisingly limited influence on ionic transport in reinforced saloplastic membranes.

Several factors may contribute to the weak dependence of ionic conductivity on reinforcement open area. First, membranes reinforced with lower open area fabrics exhibit a more uneven, corrugated structure on both the top and bottom surfaces (Fig. S5), leading to local thickness variations and a more complex transport geometry. Because membrane thickness is measured using a micrometer, which records the maximum thickness, such corrugation can lead to an overestimation of the thickness used for normalisation and, consequently, an overestimation of the calculated ionic conductivity. In addition, lower open area reinforcements increase the interfacial area between the PEC and the reinforcement, which may promote the formation of local voids or shortened transport pathways at the PEC-reinforcement interface (Fig. 7c).

Further insight into the transport behaviour is provided by water transport measurements. The membrane reinforced with the lowest open area fabric (PEEK, 71 μm, 22%) exhibits a substantially higher water flux (70 ± 15 mL m^{-2} h^{-1}) than the membrane reinforced with a more open fabric (PEEK, 40 μm, 70%), which has a water flux of 28 ± 5 mL m^{-2} h^{-1}. This suggests that transport within the PEC-reinforcement region is not uniform, but that an additional interfacial transport region may exist where the swollen PEC contacts the rigid reinforcement, *i.e.* the interfacial region (Fig. 7c). In membranes with lower open area fabrics, the relative fraction of this interfacial region is increased, which may contribute to enhanced water and ion transport. This provides a possible explanation why reductions in reinforcement open area have only a modest impact on overall ionic conductivity. A more detailed investigation of ion and water transport within the PEC-reinforcement composite region, including the role of tortuosity and interfacial area, remains an interesting topic for future work.

While tensile strength and ionic conductivity provide important insight into membrane durability and transport behaviour, the overall electrochemical performance is ultimately defined by area resistance and permselectivity.[2,3] Fig. 11b therefore compares the area resistance and permselectivity of the improved reinforced saloplastic membranes. Because all membranes were fabricated using identical processing conditions, the PEC top layer is very thin and the membrane thickness is primarily determined by the reinforcement fabric. As a result, area resistance correlates strongly with reinforcement thickness. The lowest area resistance, 2.3 ± 0.1 Ω cm^2, is obtained for the membrane reinforced with the thinnest and most open fabric (PEEK, 40 μm, 70%), which has a wet membrane thickness of only 70 μm.

This represents a substantial improvement compared to non-reinforced PSS-PDADMAC saloplastic membranes.[12,19] Previously, further reduction in membrane thickness was not possible due to insufficient mechanical stability, leading to severe stretching and deformation during testing.[19] Reinforcement enabled the fabrication of thinner membranes that retain their shape under test conditions (Fig. S4), allowing

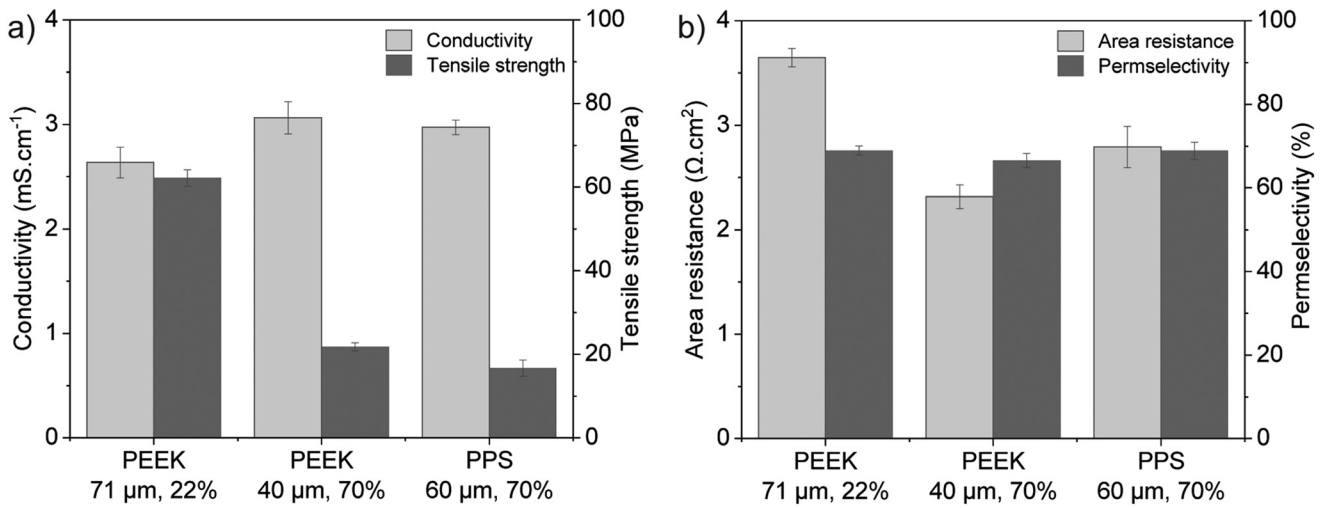

Fig. 11 Performance of reinforced saloplastic AEMs fabricated using thin, chemically stable woven reinforcements and PEC equilibrated in 0.7 M KBr. (a) Tensile strength and ionic conductivity and (b) area resistance and permselectivity, for membranes labelled by reinforcement material, fabric thickness and open area. Error bars represent the 95% confidence interval (n = 5).

the resistance contribution of the non-conductive reinforcement to be compensated by the reduction in membrane thickness. As a result, the achieved area resistances are comparable to those of some commercial AEMs measured under similar conditions, such as Neosepta AHA (4.1 Ω cm^2) and Selemion AMVN (2 Ω cm^2).[49,50]

While commercial AEMs typically exhibit higher permselectivities (>90% in 0.1/0.5 M KCl), the saloplastic membranes show lower permselectivity under these conditions due to their higher swelling and lower fixed charge density.[19] However, at lower concentration gradients (0.05/0.1 M KCl), the saloplastic membranes also exhibit high permselectivity (>90%), highlighting the importance of matching membrane properties to the intended application. Moreover, as shown in section 3.2, permselectivity can be partially tuned by adjusting PEC layer thickness, providing flexibility to tailor membrane properties to specific applications.

Overall, these results demonstrate that the trade-offs identified in the preceding sections can be effectively managed through appropriate selection of reinforcement structure and membrane thickness. In reinforced saloplastic AEMs, substantial improvements in mechanical stability can be achieved while maintaining low area resistance and largely unchanged permselectivity. This highlights reinforcement as a powerful design tool for tuning the performance of saloplastic IEMs according to application requirements. Future work will focus on evaluating long-term stability under relevant electrochemical operating conditions to further assess the durability of these membranes.

4. Conclusion

This study shows that mechanical reinforcement is an effective way to improve the performance of PSS-PDADMAC saloplastic AEMs. A spacer-free hot-pressing approach is introduced, in which the conventional spacers used in previous studies are removed, representing a new processing strategy for saloplastic IEMs. This enables direct integration of hydrated PEC with woven mesh supports. Compared to spacer-defined hot-pressing, this configuration allows the overall membrane thickness to be tuned through the combined effects of reinforcement geometry and salt-induced plasticisation of the PEC, which controls its apparent viscosity and thus the resulting PEC layer thickness. This approach enabled the fabrication of thin, mechanically stable, and defect-free membranes with low area resistance and permselectivity comparable to that of non-reinforced membranes.

Reinforcement significantly enhanced mechanical strength and dimensional stability, allowing the fabrication of much thinner membranes compared to the non-reinforced saloplastic films. Although the incorporation of a non-conductive support reduced the conductivity of the membrane, this was offset by the reduced membrane thickness, resulting in lower area resistances than those of thicker, weaker non-reinforced membranes. However, ionic conductivity did not scale linearly with the PEC content, *i.e.* PEC-reinforcement ratio. To better understand this behaviour, a series resistance model was used, supporting the presence of two distinct transport regions: a conductive dense PEC layer and a less conductive PEC-reinforcement composite region. Transport in the composite region is likely complex, as ions must move around the reinforcement, and interfacial regions between the rigid reinforcement and the swollen PEC may provide faster or alternative pathways for ion transport.

Changing the reinforcement open area showed that a lower open area leads to much higher mechanical strength, with only a modest reduction in ionic conductivity. This limited impact suggests that interfacial regions play an important role, as decreasing open area increases the relative interfacial area within the PEC-reinforcement region. These regions may contain voids or provide shorter transport pathways that facilitate ion and water transport, partially compensating for the reduced conductive area. At the same time, the presence of a continuous dense PEC layer ensures that membrane integrity and selectivity are maintained.

Despite the improved dimensional stability, permselectivity remained similar to that of non-reinforced saloplastic AEMs. This is related to the high swelling of the PEC. Reinforcement was expected to reduce swelling and improve permselectivity, but this effect was not observed. Further improvements may therefore require additional strategies, such as chemical crosslinking, although this remains challenging for the PSS-PDADMAC system.

Overall, the results show that the trade-offs between mechanical stability, area resistance and permselectivity in saloplastic AEMs can be effectively managed through careful selection of reinforcement architecture and membrane thickness. Reinforcement enabled the fabrication of thin, defect-free membranes with high mechanical stability and area resistances comparable to commercial AEMs, representing a clear advancement in the performance of saloplastic membranes for electrochemical applications.

Conflicts of interest

There are no conflicts of interest to declare.

Data availability

The data underlying this publication will be made publicly available *via* the 4TU data repository (https://data.4tu.nl/).

Supplementary information (SI) is available. See DOI: https://doi.org/10.1039/d6lp00113k.

Acknowledgements

This work is part of the intensified electrocatalytic production of hydrogen peroxide (HYPER) consortium, the consortium partners of WUR, Solvay and WFBR are thanked for the valuable discus-

sions. This project is sponsored by the Dutch Science Foundation NWO under grant number NWA.1237.18.007.

The authors gratefully acknowledge Ineke Punt for her assistance with SEM imaging.

References

1 H. Strathmann, *Ion-exchange membrane separation processes*, Elsevier, Amsterdam, 1st edn, 2004.
2 D. Kitto and J. Kamcev, The need for ion-exchange membranes with high charge densities, *J. Membr. Sci.*, 2023, **677**, 121608, DOI: 10.1016/j.memsci.2023.121608.
3 S. X. Jiang, H. S. Sun, H. J. Wang, B. P. Ladewig and Z. L. Yao, A comprehensive review on the synthesis and applications of ion exchange membranes, *Chemosphere*, 2021, **282**, 130817, DOI: 10.1016/j.chemosphere.2021.130817.
4 F. M. Allioux, L. He, F. H. She, P. D. Hodgson, L. X. Kong and L. F. Dumée, Investigation of hybrid ion-exchange membranes reinforced with non-woven metal meshes for electro-dialysis applications, *Sep. Purif. Technol.*, 2015, **147**, 353–363, DOI: 10.1016/j.seppur.2015.03.007.
5 A. Amel, S. B. Smedley, D. R. Dekel, M. A. Hickner and Y. Ein-Eli, Characterization and Chemical Stability of Anion Exchange Membranes Cross-Linked with Polar Electron-Donating Linkers, *J. Electrochem. Soc.*, 2015, **162**, F1047–F1055, DOI: 10.1149/2.0891509jes.
6 K. Chand and O. Paladino, Recent developments of membranes and electrocatalysts for the hydrogen production by Anion Exchange Membrane Water Electrolysers: A review, *Arabian J. Chem.*, 2022, 1–57, DOI: 10.1016/j.arabjc.2022.104451.
7 E. Gülzow, Alkaline fuel cells: a critical view, *J. Power Sources*, 1996, **61**, 99–104, DOI: 10.1016/S0378-7753(96)02344-0.
8 W. Jenseit, A. Khalil and H. Wendt, Material properties and processing in the production of fuel cell components: I. Hydrogen anodes from RANEY® nickel for lightweight alkaline fuel cells, *J. Appl. Electrochem.*, 1990, **20**, 893–900, DOI: 10.1007/BF01019562.
9 Q. Li, A. Molina Villarino, C. R. Peltier, A. J. Macbeth, Y. Yang, M.-J. Kim, Z. Shi, M. R. Krumov, C. Lei, G. G. Rodríguez-Calero, J. Soto, S.-H. Yu, P. F. Mutolo, L. Xiao, L. Zhuang, D. A. Muller, G. W. Coates, P. Zelenay and H. D. Abruña, Anion Exchange Membrane Water Electrolysis: The Future of Green Hydrogen, *J. Phys. Chem. C*, 2023, **127**, 7901–7912, DOI: 10.1021/acs.jpcc.3c00319.
10 D. Henkensmeier, M. Najibah, C. Harms, J. Zitka, J. Hnát and K. Bouzek, Overview: State-of-the Art Commercial Membranes for Anion Exchange Membrane Water Electrolysis, *J. Electrochem. Energy Convers. Storage*, 2021, **18**, 024001, DOI: 10.1115/1.4047963.
11 C. G. Arges and V. Ramani, Two-dimensional NMR spectroscopy reveals cation-triggered backbone degradation in polysulfone-based anion exchange membranes, *Proc. Natl. Acad. Sci. U. S. A.*, 2013, **110**, 2490–2495, DOI: 10.1073/pnas.1217215110.
12 A. B. Krishna, S. Lindhoud and W. M. de Vos, Hot-pressed polyelectrolyte complexes as novel alkaline stable monovalent-ion selective anion exchange membranes, *J. Colloid Interface Sci.*, 2021, **593**, 11–20, DOI: 10.1016/j.jcis.2021.02.077.
13 A. B. Krishna, W. M. de Vos and S. Lindhoud, Control over Charge Density by Tuning the Polyelectrolyte Type and Monomer Ratio in Saloplastic-Based Ion-Exchange Membranes, *Langmuir*, 2023, **39**, 6874–6884, DOI: 10.1021/acs.langmuir.3c00497.
14 C. H. Porcel and J. B. Schlenoff, Compact Polyelectrolyte Complexes: "Saloplastic" Candidates for Biomaterials, *Biomacromolecules*, 2009, **10**, 2968–2975, DOI: 10.1021/bm900373c.
15 P. Schaaf and J. B. Schlenoff, Saloplastics: Processing Compact Polyelectrolyte Complexes, *Adv. Mater.*, 2015, **27**, 2420–2432, DOI: 10.1002/adma.201500176.
16 A. B. Krishna, J. D. Willott, S. Lindhoud and W. M. de Vos, Hot-pressing polyelectrolyte complexes into tunable dense saloplastics, *Polymer*, 2022, **242**, 124583, DOI: 10.1016/j.polymer.2022.124583.
17 J. Y. Li, L. J. Li, H. A. Brink, G. Allegri and S. Lindhoud, Polyelectrolyte complex-based materials for separations: progress, challenges and opportunities, *Mater. Horiz.*, 2025, **12**, 4889–5030, DOI: 10.1039/d4mh01840k.
18 R. F. Shamoun, A. Reisch and J. B. Schlenoff, Extruded Saloplastic Polyelectrolyte Complexes, *Adv. Funct. Mater.*, 2012, **22**, 1923–1931, DOI: 10.1002/adfm.201102787.
19 H. A. Brink, R. P. Martinho, W. M. de Vos and S. Lindhoud, Improving the fixed charge density of sustainably produced saloplastic anion exchange membranes, *RSC Sustainability*, 2025, **3**, 3473–3482, DOI: 10.1039/d5su00221d.
20 X. Y. Luo, D. I. Kushner and A. Kusoglu, Anion exchange membranes: The effect of reinforcement in water and electrolyte, *J. Membr. Sci.*, 2023, **685**, 121945, DOI: 10.1016/j.memsci.2023.121945.
21 I. R. Chowdhury and J. Summerscales, Woven Fabrics for Composite Reinforcement, *Rev. J. Compos. Sci.*, 2024, **8**, 280, DOI: 10.3390/jcs8070280.
22 R. Qelibari, E. C. Ortiz, N. van Treel, F. Lombeck, C. Schare, A. Münchinger, N. Dumbadze, G. Titvinidze, C. Klose and S. Vierrath, 74 μm PEEK-Reinforced Sulfonated Poly(phenylene sulfone)-Membrane for Stable Water Electrolysis with Lower Gas Crossover and Lower Resistance than Nafion N115, *Adv. Energy Mater.*, 2024, **14**, 2303271, DOI: 10.1002/aenm.202303271.
23 E. Stránská and D. Neděla, Reinforcing fabrics as the mechanical support of ion exchange membranes, *J. Ind. Text.*, 2018, **48**, 432–447, DOI: 10.1177/1528083717732075.
24 C. Boaretti, L. Pasquini, R. Sood, S. Giancola, A. Donnadio, M. Roso, M. Modesti and S. Cavaliere, Mechanically stable nanofibrous sPEEK/Aquivion composite membranes for fuel cell applications, *J. Membr. Sci.*, 2018, **545**, 66–74, DOI: 10.1016/j.memsci.2017.09.055.
25 M. Najibah, J. Hnát, M. Plevová, A. Dayan, J. Stojadinovic, J. Žitka, C. Bae, K. Bouzek and D. Henkensmeier, PPS-

reinforced poly(terphenylene) anion-exchange membranes with different quaternary ammonium groups for use in water electrolysers, *J. Membr. Sci.*, 2025, **713**, 123335, DOI: 10.1016/j.memsci.2024.123335.

26 L. Hernández-Pérez, M. C. Martí-Calatayud, M. T. Montañés and V. Pérez-Herranz, Interplay between Forced Convection and Electroconvection during the Overlimiting Ion Transport through Anion-Exchange Membranes: A Fourier Transform Analysis of Membrane Voltage Drops, *Membranes*, 2023, **13**, 363, DOI: 10.3390/membranes13030363.

27 J. Krivcík, D. Nedela and R. Válek, Ion-exchange membrane reinforcing, *Desalin. Water Treat.*, 2015, **56**, 3214–3219, DOI: 10.1080/19443994.2014.981411.

28 S. Hommura, Y. Kunisa, I. Terada and M. Yoshitake, Characterization of fibril reinforced membranes for fuel cells, *J. Fluorine Chem.*, 2003, **120**, 151–155, DOI: 10.1016/S0022-1139(02)00324-X.

29 L. Liu, H. B. Li and G. Avgouropoulos, A review of porous polytetrafluoroethylene reinforced sulfonic acid-based proton exchange membranes for fuel cells, *Int. J. Hydrogen Energy*, 2024, **50**, 501–527, DOI: 10.1016/j.ijhydene.2023.08.270.

30 H.-N. Moon, H.-B. Song and M.-S. Kang, Thin Reinforced Ion-Exchange Membranes Containing Fluorine Moiety for All-Vanadium Redox Flow Battery, *Membranes*, 2021, **11**, 867, DOI: 10.3390/membranes11110867.

31 M. L. Lehmann, L. Tyler, E. C. Self, G. Yang, J. Nanda and T. Saito, Membrane design for non-aqueous redox flow batteries: Current status and path forward, *Chem*, 2022, **8**, 1611–1636, DOI: 10.1016/j.chempr.2022.04.005.

32 S. Banerjee, D. N. Prugh and S. Frisk, Advances in Proton Exchange Membrane Technology, *ECS Trans.*, 2013, **50**, 887–895, DOI: 10.1149/05002.0887ecst.

33 F. Eckert, Polyamide Fabrics (PA) – Technical Data, (n.d.). https://www.franz-eckert.de/polyamide-fabrics.html (accessed January 28, 2026).

34 Sefar Group, Fabrics for the Reinforcement, (n.d.). https://hello.sefar.com/iem (accessed January 28, 2026).

35 H. Khalid, M. Najibah, H. S. Park, C. Bae and D. Henkensmeier, Properties of Anion Exchange Membranes with a Focus on Water Electrolysis, *Membranes*, 2022, **12**, 12100989, DOI: 10.3390/membranes12100989.

36 ASTM, ASTM D882, Standard Test Method for Tensile Properties of Thin Plastic Sheeting, 2018.

37 J. J. Krol, M. Wessling and H. Strathmann, Concentration polarization with monopolar ion exchange membranes: current-voltage curves and water dissociation, *J. Membr. Sci.*, 1999, **162**, 145–154, DOI: 10.1016/S0376-7388(99)00133-7.

38 A. H. Galama, N. A. Hoog and D. R. Yntema, Method for determining ion exchange membrane resistance for electrodialysis systems, *Desalination*, 2016, **380**, 1–11, DOI: 10.1016/j.desal.2015.11.018.

39 Q. Lin, X. Sun, X. Chen and S. Shi, Effect of Pretreatment on Microstructure and Mechanical Properties of NafionTM XL Composite Membrane, *Fuel Cells*, 2019, **19**, 530–538, DOI: 10.1002/fuce.201900064.

40 Y. Tang, A. Kusoglu, A. M. Karlsson, M. H. Santare, S. Cleghorn and W. B. Johnson, Mechanical properties of a reinforced composite polymer electrolyte membrane and its simulated performance in PEM fuel cells, *J. Power Sources*, 2008, **175**, 817–825, DOI: 10.1016/j.jpowsour.2007.09.093.

41 S. Porada, W. J. Van Egmond, J. W. Post, M. Saakes and H. V. M. Hamelers, Tailoring ion exchange membranes to enable low osmotic water transport and energy efficient electrodialysis, *J. Membr. Sci.*, 2018, **552**, 22–30, DOI: 10.1016/j.memsci.2018.01.050.

42 F. G. Helfferich, *Ion exchange*, Dover Publications, New York, 1995.

43 R. M. DuChanois, M. Heiranian, J. Yang, C. J. Porter, Q. Li, X. Zhang, R. Verduzco and M. Elimelech, Designing polymeric membranes with coordination chemistry for high-precision ion separations, *Sci. Adv.*, 2022, **8**, eabm9436, DOI: 10.1126/sciadv.abm9436.

44 H. Fan and N. Y. Yip, Elucidating conductivity-permselectivity tradeoffs in electrodialysis and reverse electrodialysis by structure-property analysis of ion-exchange membranes, *J. Membr. Sci.*, 2019, **573**, 668–681, DOI: 10.1016/j.memsci.2018.11.045.

45 A. Zlotorowicz, R. V. Strand, O. S. Burheim, Ø. Wilhelmsen and S. Kjelstrup, The permselectivity and water transference number of ion exchange membranes in reverse electrodialysis, *J. Membr. Sci.*, 2017, **523**, 402–408, DOI: 10.1016/j.memsci.2016.10.003.

46 S. B. B. Solberg, Ø. Wilhelmsen and O. S. Burheim, Transport numbers of ion-exchange membranes in ternary mixtures of KCl, H_2O and ethanol relevant for electrodialysis and desalination processes, *Electrochim. Acta*, 2024, **506**, 145018, DOI: 10.1016/j.electacta.2024.145018.

47 J.-H. Choi, S.-H. Kim and S.-H. Moon, Heterogeneity of Ion-Exchange Membranes: The Effects of Membrane Heterogeneity on Transport Properties, *J. Colloid Interface Sci.*, 2001, **241**, 120–126, DOI: 10.1006/jcis.2001.7710.

48 M. Seo, W. Kim, H. Lee and S. J. Kim, Non-negligible effects of reinforcing structures inside ion exchange membrane on stabilization of electroconvective vortices, *Desalination*, 2022, **538**, 115902, DOI: 10.1016/j.desal.2022.115902.

49 Astom Corporation, Ion Exchange Membrane, (n.d.). https://www.astom-corp.jp/en/product/10.html (accessed January 28, 2026).

50 AGC, Ion-exchange membrane SELEMION, 2026. https://www.agec.co.jp/eng/product/selemion/membrane.html (accessed January 28, 2026).